

Suppression of superconductivity by the localization of hole carriers in Ti-doped $\text{La}_{1.85}\text{Sr}_{0.15}\text{CuO}_4$

Caixia Wang,¹ Yuping Sun,¹ Zhe Qu,² and Yuheng Zhang^{1,2,*}

¹Key Laboratory of Materials Physics, Institute of Solid State Physics, Chinese Academy of Sciences, Hefei 230031, People's Republic of China

²Hefei High Magnetic Field Laboratory, University of Science and Technology of China, Hefei 230026, People's Republic of China

(Received 21 October 2005; revised manuscript received 19 January 2006; published 28 April 2006)

The effects of Ti doping in the single-doped samples of $\text{La}_{1.85}\text{Sr}_{0.15}\text{Cu}_{1-x}\text{Ti}_x\text{O}_4$ ($0 \leq x \leq 0.06$) and the double-doped samples of $\text{La}_{1.85-2x}\text{Sr}_{0.15+2x}\text{Cu}_{1-x}\text{Ti}_x\text{O}_4$ ($0 \leq x \leq 0.4$) have been studied. The critical Ti doping level (above which the pure phase is not formed) of double-doped samples are much higher than that of the single-doped samples. For single-doped samples, the high valence Ti^{4+} would introduce extra electrons into the CuO_2 plane, which leads to severe valence mismatch and prevents the formation of a pure phase sample at $x > 0.06$ and the superconductivity is depressed at $x > 0.04$. While for double-doped samples, the extra electrons introduced by the doping of Ti are compensated by increasing holes due to the increase of the Sr content, which lead to the valence balance in the system. Thus, the pure-phase samples are formed up to $x=0.4$ and the superconductivity can survive up to $x=0.1$. The resistivity for double-doped samples is three orders of magnitude smaller than that for single-doped samples at the same Ti doping content. The reason that Ti dopants suppress superconductivity is attributed to the localization of hole carriers.

DOI: [10.1103/PhysRevB.73.144518](https://doi.org/10.1103/PhysRevB.73.144518)

PACS number(s): 74.72.Dn, 74.20.Mn, 74.25.Ha

I. INTRODUCTION

The discovery of superconductivity in doped La_2CuO_4 by Bednorz and Müller has attracted much renewed attention.¹ Recently in conventional superconductors, a magnetic impurity is found to be most destructive to superconductivity due to the magnetic pair-breaking effect. While in high-temperature superconductors, many authors²⁻⁵ believed that the magnetism can coexist with superconductivity. The characteristics of the CuO_2 plane have proven to be key issues in understanding the high temperature superconductivity. The 3d transition metal elements doping on the CuO_2 plane can offer opportunities for studying the interplay between magnetism and superconductivity. Due to the simplest layered structure of the La_2CuO_4 system, attempts have been made to substitute a great variety of transition metals or other elements for copper in $\text{La}_{1.85}\text{Sr}_{0.15}\text{CuO}_4$.⁶⁻¹⁴ A common result in all of these studies is that T_c is depressed in the same manner, independent of whether the dopant is magnetic or nonmagnetic.

Up to now the mechanism of high- T_c superconductivity has not yet been fully understood. Moreover it is still controversial whether magnetic dopants are the crucial origin of destroying superconductivity alike for the conventional superconductor. As is well known, the Zn substitution for in-plane Cu sites destroys the superconductivity quite rapidly in contrast to the other transition metal substitutions such as Ni.³ Consequently, the mechanism of the suppressed superconductivity by Zn doping is supposed that Zn impurity induces staggered magnetic moments on the Cu site around the impurity, which causes pair breaking, while leaving the carrier concentration in the CuO_2 plane unaltered. But these researches are all bases on light-doped samples. Even for the nonmagnetic cation Zn^{2+} , the superconductivity is completely suppressed by only a few percent of impurity (<0.1). Additionally, Zn^{2+} and

Cu^{2+} have the same valence, which cause the carrier concentration in the CuO_2 plane to remain unaltered. However, a high-valence metal doping would lead to a change of carrier concentration in the CuO_2 plane. It is well known that high- T_c superconductivity is sensitive to the carrier concentration in the CuO_2 plane. Thus, the study of high-valence nonmagnetic cation doping (such as Ti^{4+}) is important in efforts to understand the mechanism of the depression of superconductivity resulting from transitional metal doping.

In a previous study we have investigated high-valence Mn ion substitution for Cu sites in the $\text{La}_{1.85}\text{Sr}_{0.15}\text{CuO}_4$ system, where the double-doped $\text{La}_{1.85-2x}\text{Sr}_{0.15+2x}\text{Cu}_{1-x}\text{Mn}_x\text{O}_4$ samples were used.⁴ A double-doped process can be employed to nearly compensate for the strong decrease of carrier concentration induced by high-valence ion doping, to keep the carrier concentration constant. In this paper, we have chosen the Ti^{4+} ion as the doping element for the Cu ion because it has no 3d electron and it is a nonmagnetic ion. For Ti-doped samples of $\text{La}_{1.85}\text{Sr}_{0.15}\text{Cu}_{1-x}\text{Ti}_x\text{O}_4$, x-ray diffraction analysis reveals that the pure phase samples can be obtained only at doping levels $x \leq 0.06$. Thus we perform a double-doping experiment and successfully synthesize the doubly doped samples of $\text{La}_{1.85-2x}\text{Sr}_{0.15+2x}\text{Cu}_{1-x}\text{Ti}_x\text{O}_4$ ($0 \leq x \leq 0.4$) with good single phase. This is attributed to the carrier compensation effect¹⁵ in which extra electrons introduced by the substitution of high valence Ti^{4+} for Cu^{2+} are compensated by the increasing holes due to the Sr^{2+} substitution for La^{3+} . Therefore, the Ti doping level for double-doped samples is much higher than that for the single-doped samples and the superconductivity can survive up to $x=0.1$ for double-doped samples while $x=0.04$ for single-doped samples. The suppression of superconductivity is suggested to originate from the localization of the hole carriers.

II. EXPERIMENT

Polycrystalline samples of $\text{La}_{1.85}\text{Sr}_{0.15}\text{Cu}_{1-x}\text{Ti}_x\text{O}_4$ ($x=0, 0.02, 0.04, 0.06$) and $\text{La}_{1.85-2x}\text{Sr}_{0.15+2x}\text{Cu}_{1-x}\text{Ti}_x\text{O}_4$ ($x=0.00, 0.02, 0.04, 0.06, 0.08, 0.1, 0.11, 0.15, 0.2, 0.3, 0.4$) were synthesized by means of a conventional solid state reaction method using appropriate powders of La_2O_3 , SrCO_3 , TiO_2 , and CuO . The powders were mixed and pre-fired several times in air at 900°C for a total period of about 36 h with a few intermediate grindings. The pre-fired materials were mixed and pressed into a pellet, followed by sintering in air at $1120\text{--}1230^\circ\text{C}$ for 24 h.

X-ray diffraction (XRD) analysis was carried out using a Philips X'Pert Pro x-ray diffractometer with $\text{Cu } K\alpha$ radiation at room temperature to screen for the presence of impurity phase and the changes in structure. The lattice parameters were obtained by Rietveld refinement of the x-ray patterns. The resistance was measured using the standard four-probe method in a commercial Physical Property Measurement System (PPMS, $1.8\text{ K} \leq T \leq 400\text{ K}$, $0\text{ T} \leq H \leq 9\text{ T}$) from 5 to 300 K. The magnetic measurement was performed on a Quantum Design superconducting quantum interference device (SQUID) MPMS system under zero-field cooled (ZFC) mode for all samples in the temperature range from 5 to 300 K. For the $\text{La}_{1.85-2x}\text{Sr}_{0.15+2x}\text{Cu}_{1-x}\text{Ti}_x\text{O}_4$ ($x=0.1$) sample, ZFC magnetization measurement and field-cooled (FC) magnetization measurements were carried out in the temperature range from 5 to 50 K. The infrared (IR) transmission spectra were obtained (MAGNA-IR 750) using powder samples with KBr serving as a carrier over the frequency range $400\text{--}800\text{ cm}^{-1}$. The morphologies of these samples were investigated by the Scion200 scanning electron microscope (SEM).

III. RESULTS AND DISCUSSION

A. Structure

We obtain pure phase samples of $\text{La}_{1.85}\text{Sr}_{0.15}\text{Cu}_{1-x}\text{Ti}_x\text{O}_4$ at doping levels $x \leq 0.06$. Above this level, impurities emerge due to the fact that doping with Ti^{4+} cations at Cu^{2+} cations will lead to valence unbalance, which gives rise to preventing the preparation of pure-phase samples. In order to maintain the valence balance and achieve high doping level, we used the double-doped method, namely, the valence decrease that the increase in Sr^{2+} concentration and the decrease in La^{3+} concentration balances out the increasing valence due to the substitution of Ti^{4+} for Cu^{2+} . By virtue of the double-doped technique, we successfully synthesized pure phase samples with $\text{La}_{1.85-2x}\text{Sr}_{0.15+2x}\text{Cu}_{1-x}\text{Ti}_x\text{O}_4$ ($0 \leq x \leq 0.4$).

XRD analysis shows that the samples of $\text{La}_{1.85}\text{Sr}_{0.15}\text{Cu}_{1-x}\text{Ti}_x\text{O}_4$ ($x=0, 0.02, 0.04, 0.06$) and $\text{La}_{1.85-2x}\text{Sr}_{0.15+2x}\text{Cu}_{1-x}\text{Ti}_x\text{O}_4$ ($x=0.00, 0.02, 0.04, 0.06, 0.08, 0.1, 0.11, 0.15, 0.2, 0.3, 0.4$) are all crystallized in a single-phase tetragonal lattice with the space group $I4/mmm$, as shown in Figs. 1 and 2. The lattice parameters can be obtained by fitting the experimental spectra using the standard Rietveld technique.¹⁶ The obtained lattice parameters are shown in Figs. 3 and 4, respectively. Clearly, with increasing Ti doping, the lattice parameter a increases monotonously,

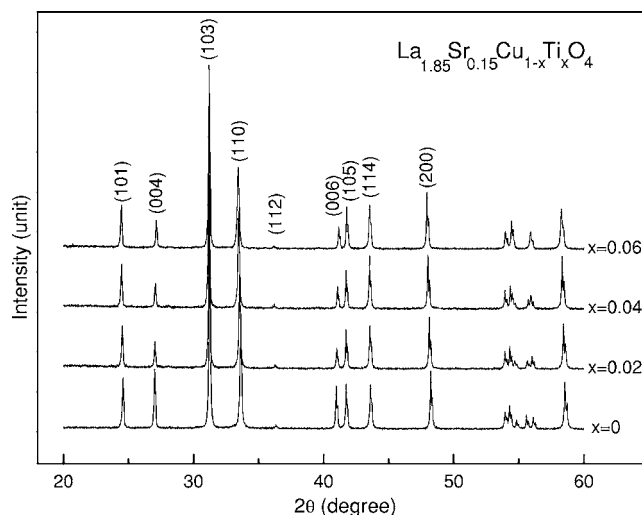


FIG. 1. The XRD patterns of $\text{La}_{1.85}\text{Sr}_{0.15}\text{Cu}_{1-x}\text{Ti}_x\text{O}_4$.

while c decreases. In addition, a monotonous decrease in c/a can be seen in Figs. 3 and 4. The c/a ratio is commonly used to characterize the Jahn-Teller distortion of the oxygen octahedron around Cu^{2+} . It is obvious that Ti doping releases the Jahn-Teller distortion of the CuO_6 octahedron. In order to prove the homogeneity of these samples, the morphologies of these samples were investigated with the Scion200 scanning electron microscope (SEM). In Fig. 5, the SEM photograph shows that the grains are densely and regularly arranged, which indicates that the Ti^{4+} ions are distributed homogeneously in $\text{La}_{1.85-2x}\text{Sr}_{0.15+2x}\text{Cu}_{1-x}\text{Ti}_x\text{O}_4$ and no segregation of the secondary phase is observed.

We obtain pure phase samples of $\text{La}_{1.85}\text{Sr}_{0.15}\text{Cu}_{1-x}\text{Ti}_x\text{O}_4$ at doping levels of $x \leq 0.06$, which by virtue of the double-doped technique, the pure phase samples can be obtained up to $x=0.4$. In order to further explore the doping effect of Ti, the vibration modes in the $\text{Cu}(\text{Ti})\text{O}_6$ octahedron have been investigated by means of infrared (IR) transmission measurements. Figure 6 shows the IR transmission spectra of $\text{La}_{1.85-2x}\text{Sr}_{0.15+2x}\text{Cu}_{1-x}\text{Ti}_x\text{O}_4$ ($0 \leq x \leq 0.4$) samples. According to the earlier investigation,^{17–19} the two IR modes about 503 cm^{-1} and 680 cm^{-1} in Fig. 6 are assigned to the stretching mode of apical oxygen atoms and the stretching mode of in-plane oxygen atoms, respectively. From Fig. 6 one can see that the $\nu_1=503\text{ cm}^{-1}$ peak appears in all samples, while the ν_2 peak only appears in $0.15 \leq x \leq 0.4$ samples. With increasing Ti content, the ν_1 mode slightly shifts to a high frequency while the other peak ν_2 at 680 cm^{-1} emerges and its intensity increases with x for samples with $x \geq 0.2$. Thus, based on the results of XRD and IR transmission spectra, we conclude that all samples are in a simple tetragonal phase, and the additional Sr sits only on the rare-earth sites and Ti only replaces Cu.

B. Superconductivity

Figure 7 displays the temperature dependence of magnetization for $\text{La}_{1.85}\text{Sr}_{0.15}\text{Cu}_{1-x}\text{Ti}_x\text{O}_4$ ($0 \leq x \leq 0.06$). The inset in Fig. 7 reveals the diamagnetic behavior for the sample with $x=0$. As can be seen from Fig. 7, the samples with $x=0.02$

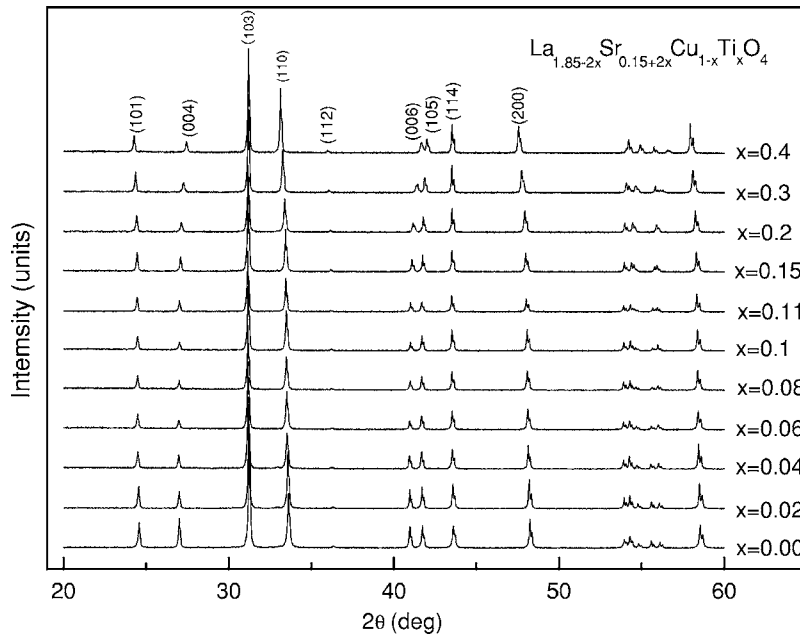


FIG. 2. The XRD patterns of $\text{La}_{1.85-2x}\text{Sr}_{0.15+2x}\text{Cu}_{1-x}\text{Ti}_x\text{O}_4$.

and 0.04 also show a diamagnetic signal and reveal the occurrence of superconductivity at about 31.0 K and 26.1 K, respectively. While there is no diamagnetism and the superconductivity is suppressed for the sample with $x=0.06$. Figure 8 gives the temperature dependence of magnetization for $\text{La}_{1.85-2x}\text{Sr}_{0.15+2x}\text{Cu}_{1-x}\text{Ti}_x\text{O}_4$ ($0 \leq x \leq 0.08$). The diamagnetism is observed for all the samples. The T_c^{onset} values are about 37 K, 32.9 K, 32.8 K, 30 K, and 30 K for samples with $x=0, 0.02, 0.04, 0.06$, and 0.08 , respectively. In the

inset of Figs. 8(a) and 8(b) we give the enlarged views around the superconducting transition. Moreover, one can clearly see that the systems are in the paramagnetic state at temperatures higher than T_c^{onset} for samples with $0.04 \leq x$

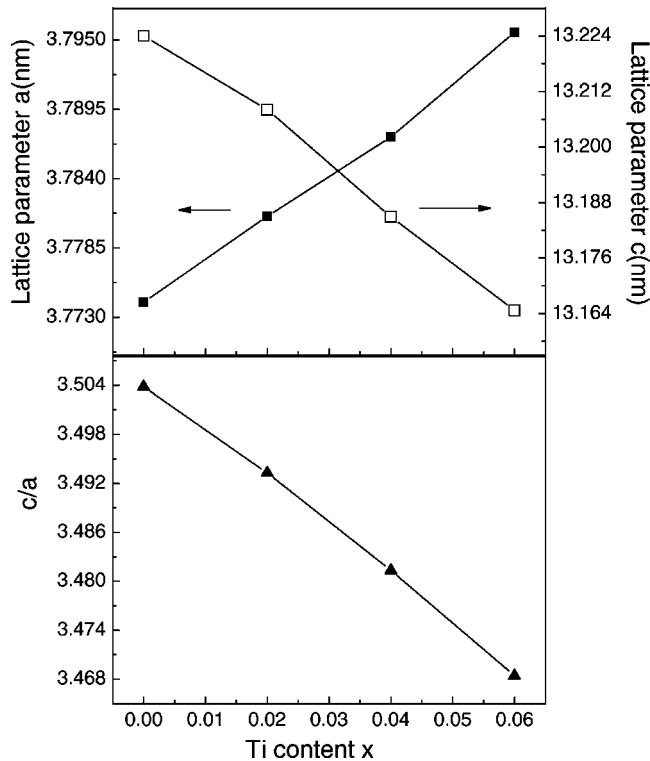


FIG. 3. Lattice parameters a and c and the ratio of c/a as a function of Ti content in the $\text{La}_{1.85}\text{Sr}_{0.15}\text{Cu}_{1-x}\text{Ti}_x\text{O}_4$ system.

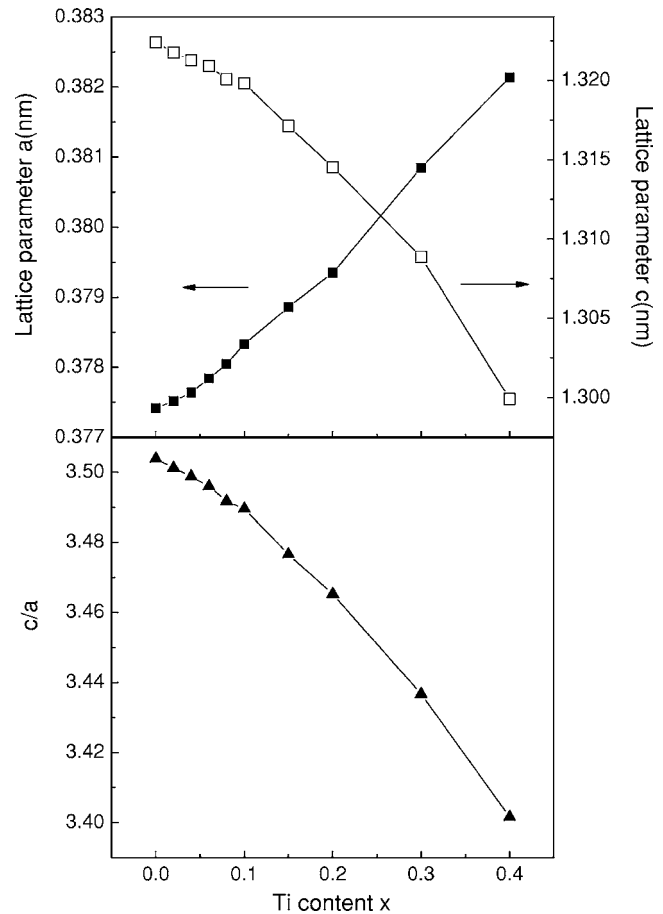


FIG. 4. Lattice parameters a and c and the ratio of c/a as a function of Ti content in the $\text{La}_{1.85-2x}\text{Sr}_{0.15+2x}\text{Cu}_{1-x}\text{Ti}_x\text{O}_4$ system.

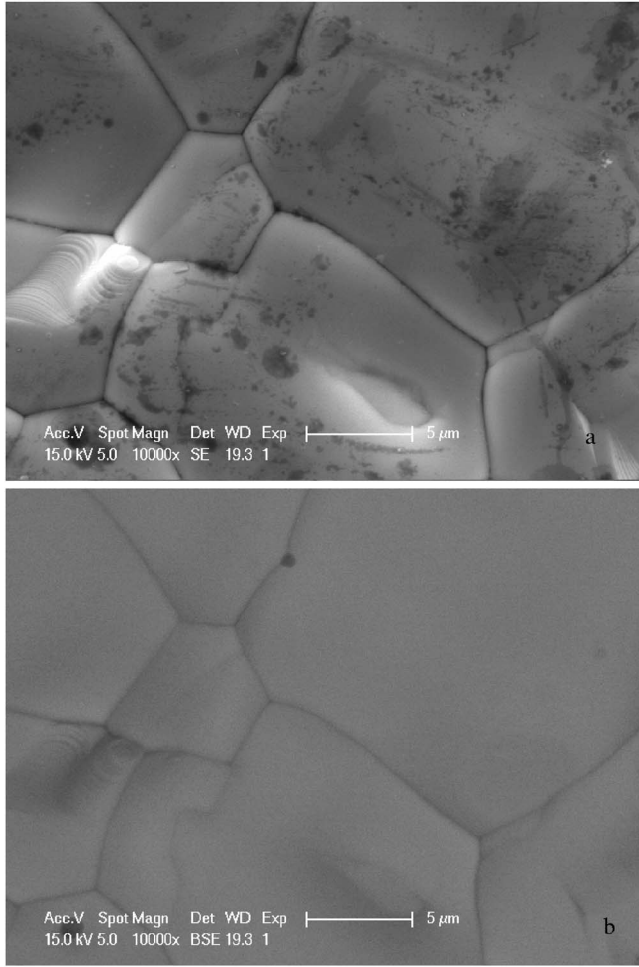


FIG. 5. SEM micrograph of a polycrystalline sample $\text{La}_{1.85-2x}\text{Sr}_{0.15+2x}\text{Cu}_{1-x}\text{Ti}_x\text{O}_4$ with $x=0.3$.

≤ 0.08 . The Meissner volume decreases sharply with increasing Ti doping content in both series of samples.

C. Coexistence and competition of superconductivity and paramagnetism

Figure 9 shows the temperature dependence of magnetization for the samples with $x=0.1, 0.11$ in the double-doped $\text{La}_{1.85-2x}\text{Sr}_{0.15+2x}\text{Cu}_{1-x}\text{Ti}_x\text{O}_4$ system. For the sample with $x=0.1$, the magnetization first presents the upturn and exhibits paramagnetic behavior with decreasing temperature until about 30 K, then it begins to decrease abruptly upon further cooling, the diamagnetic signal occurs at about 17 K and reaches a negative maximum at 11.3 K, and then it begins to increase abruptly, in which a valley is formed. In order to understand this magnetization behavior, we compared the ZFC and FC magnetization for this sample, as shown in the inset of Fig. 9(a). The applied magnetic field was 100 Oe. From the inset in Fig. 9(a) one can see that the temperature dependence of magnetization under the FC condition is similar to that under the ZFC condition except for the value of valley, which explains that the drop of the magnetic signal is attributed to the superconductive transition. For the sample with $x=0.11$, there is no diamagnetism and the superconduc-

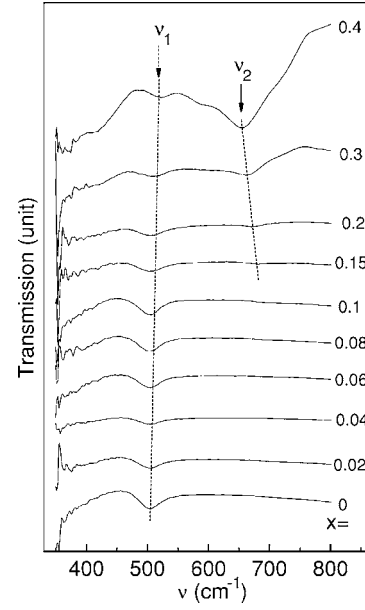


FIG. 6. The infrared transmission spectra of $\text{La}_{1.85-2x}\text{Sr}_{0.15+2x}\text{Cu}_{1-x}\text{Ti}_x\text{O}_4$ samples.

tivity is suppressed. To understand whether it is the paramagnetic behavior before and after the superconductive transition for the sample with $x=0.1$, the Brillouin function is used to fit the M - T experimental data. It is well known that the Brillouin function^{20,21} B_J describes the temperature dependence of magnetization M for the paramagnet under the external magnetic field H and the quantum number J of the magnetic ion. The Brillouin function is

$$B_J(x) = \frac{2J+1}{2J} \coth\left(\frac{(2J+1)x}{2J}\right) - \frac{1}{2J} \coth\left(\frac{x}{2J}\right), \quad (1)$$

where $x = \frac{gJ\mu_B H}{k_B T}$ (where g is spectroscopic splitting factor, μ_B is the Bohr magneton, k_B is Boltzmann's constant, and T is

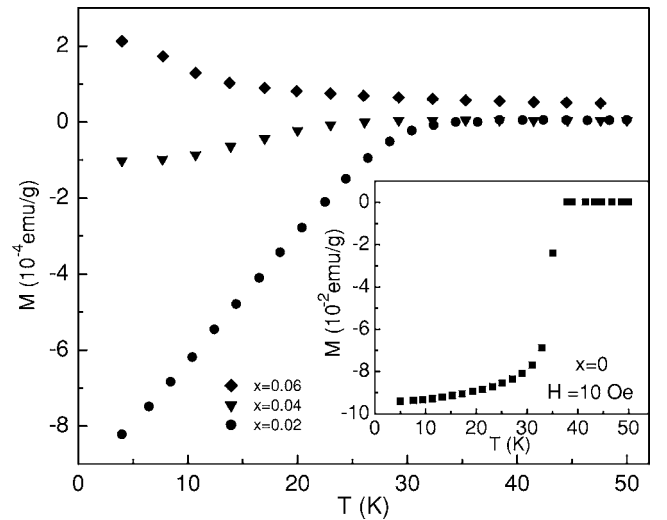


FIG. 7. The temperature dependence of the magnetization of $\text{La}_{1.85}\text{Sr}_{0.15}\text{Cu}_{1-x}\text{Ti}_x\text{O}_4$ ($0.02 \leq x \leq 0.06$). The inset of is the M - T curves of $x=0$.

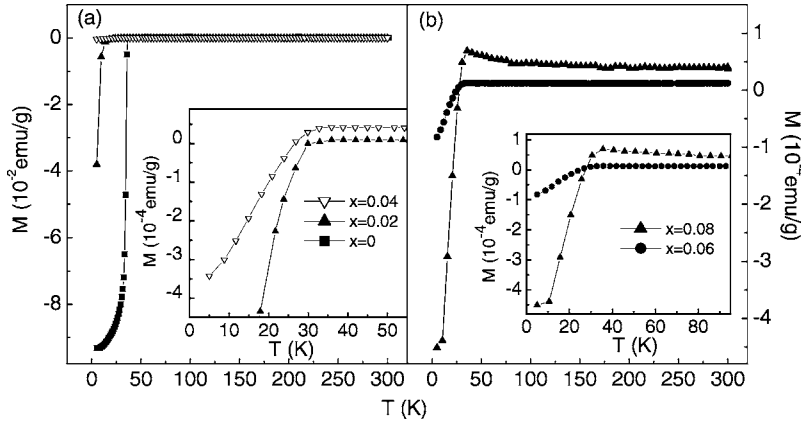


FIG. 8. The temperature dependence of the magnetization of $\text{La}_{1.85-2x}\text{Sr}_{0.15+2x}\text{Cu}_{1-x}\text{Ti}_x\text{O}_4$ ($0 \leq x \leq 0.08$). ZFC, $H=10$ Oe for samples with $0 \leq x \leq 0.06$ and $H=100$ Oe for the sample with $x=0.08$. Insets are the enlarged views around the superconducting transition.

temperature). Using the Brillouin function, the M as function of T can be described as

$$M = NgJ\mu_B B_J(x) = N\mu_{\text{eff}} B_J(x), \quad (2)$$

where N is the number of atoms with magnetism per unit volume, the effective magnetic moment μ_{eff} ($\mu_{\text{eff}} = gJ\mu_B$) is one of the fitting parameters and J is 1/2 for Cu^{2+} . Figure 9(b) displays the fitting result for the sample with $x=0.1$. The effective magnetic moment μ_{eff} can be obtained by this fitting as $1.49\mu_B$. According to a mean field approximation,²² the expected effective magnetic moment μ_{eff} is $1.56\mu_B$. The experimental effective magnetic moment is close to the calculated data. It can be seen in Fig. 9(b) that the data can fit the Brillouin function of paramagnetism very well before the superconducting transition. Below this transition, our experiment data fit the Brillouin function very well after subtracting the superconductive signal from the crude data. As a result, the coexistence and competition between the diamagnetism and paramagnetism exist in this doped system. At a low doping level, i.e., $x \leq 0.1$, the diamagnetism overwhelms the paramagnetism. Thus these samples exhibit a superconducting transition. At the doping level $0.11 \leq x \leq 0.4$, due to more and more Ti^{4+} ions being introduced into the lattice, which lead to more and more $3d$ electrons localized at Cu^{2+} ,

the paramagnetism becomes stronger and stronger and overwhelms the diamagnetism; thus the paramagnetism is exhibited at this doping range, as shown in Figs. 9 and 10

D. ρ - T relation

The temperature dependencies of resistivity for samples of $\text{La}_{1.85}\text{Sr}_{0.15}\text{Cu}_{1-x}\text{Ti}_x\text{O}_4$ and $\text{La}_{1.85-2x}\text{Sr}_{0.15+2x}\text{Cu}_{1-x}\text{Ti}_x\text{O}_4$ are shown in Figs. 11 and 12, respectively. For $\text{La}_{1.85}\text{Sr}_{0.15}\text{Cu}_{1-x}\text{Ti}_x\text{O}_4$ samples, the resistivity ρ increases dramatically with increasing Ti content. The sample with $x=0$ exhibits superconductivity at about 37 K. The resistivity of the sample with $x=0.02$ decreases gradually with decreasing temperature first and then displays an upturn; a broad dip can be observed at about 30 K. This dip reveals a weakened superconductivity as shown in the inset of Fig. 11. For the samples with $x=0.04$ and 0.06 , the ρ shows semiconductor-like behavior. For $\text{La}_{1.85-2x}\text{Sr}_{0.15+2x}\text{Cu}_{1-x}\text{Ti}_x\text{O}_4$ samples, we notice that the doping of Ti depresses the superconductivity dramatically. For $x=0.02$, the ρ decreases gradually with decreasing temperature first and then shows an upturn at about 130 K, but finally drops at 15 K and decreases gradually with further cooling. This reveals a broadened superconducting transition. For the doping level $0.04 \leq x \leq 0.08$, the resistivity exhibits metal behavior at high temperature and semi-

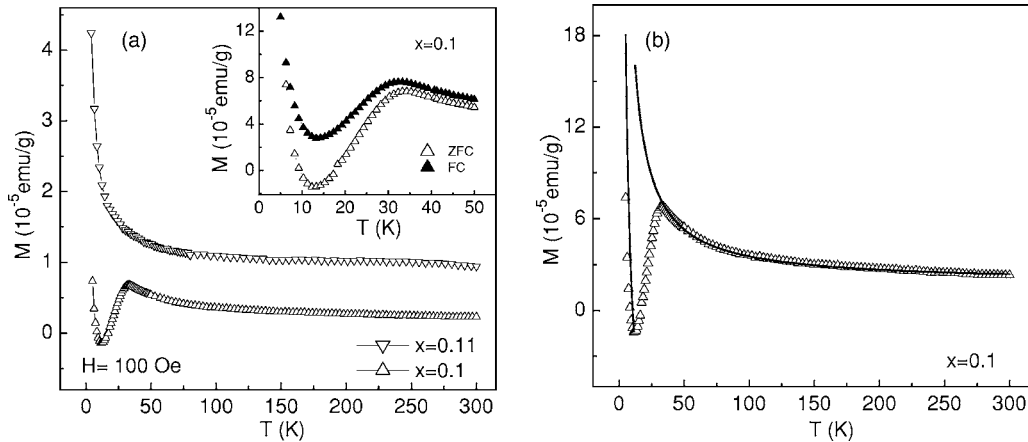


FIG. 9. (a) The temperature dependence of the magnetization of $\text{La}_{1.85-2x}\text{Sr}_{0.15+2x}\text{Cu}_{1-x}\text{Ti}_x\text{O}_4$ ($x=0.1, 0.11$). The inset is the enlarged view for $x=0.1$ around the superconducting transition. (b) The fitting results of the M - T curve for the sample with $x=0.1$ using the Brillouin function. The solid line is the fitting curve and the hollow symbols are the experimental data.

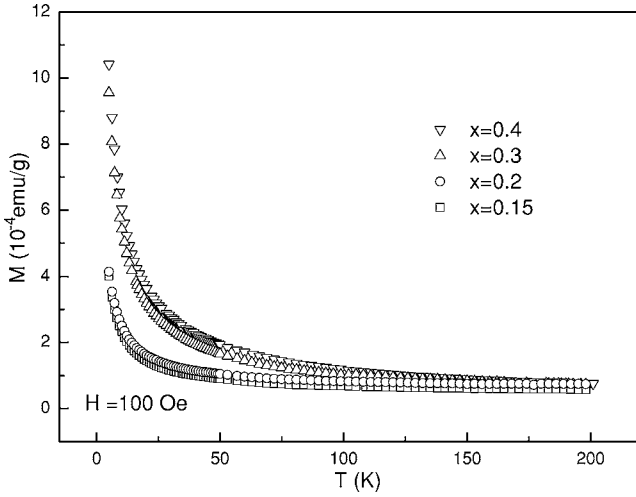


FIG. 10. The temperature dependence of the magnetization of $\text{La}_{1.85-2x}\text{Sr}_{0.15+2x}\text{Cu}_{1-x}\text{Ti}_x\text{O}_4$ ($0.15 \leq x \leq 0.4$).

conductorlike behavior at low temperature. Such a behavior has been observed in many transition-metal-doped $\text{La}_2\text{CuO}_{4+\delta}$ and $\text{YBa}_2\text{Cu}_3\text{O}_{4+\delta}$ compounds.^{6,23–26} For the doping level $0.1 \leq x \leq 0.4$, these samples show semiconductorlike behavior throughout the measured temperature regime. From Figs. 11 and 12 we can see that the resistivity increases quickly with increasing x for two kinds of samples. For example, for the $\text{La}_{1.85}\text{Sr}_{0.15}\text{Cu}_{1-x}\text{Ti}_x\text{O}_4$ samples, at about 40 K which is little higher than the T_c for $x=0$, the resistivity of $x=0.06$ is about six orders of magnitude higher than that of $x=0$. While for the $\text{La}_{1.85-2x}\text{Sr}_{0.15+2x}\text{Cu}_{1-x}\text{Ti}_x\text{O}_4$ samples, at about 40 K, the resistivity of $x=0.06$ is only one order of magnitude higher than that of $x=0$. The resistivity is larger in single-doped samples than that in double-doped samples at the same Ti doping content. We consider that the difference in normal state electrical transport is attributed to the change of the hole carrier in the CuO_2 plane for the two series of samples. In single-doped samples, the substitution of high valence Ti introduces extra electrons and leads to the de-

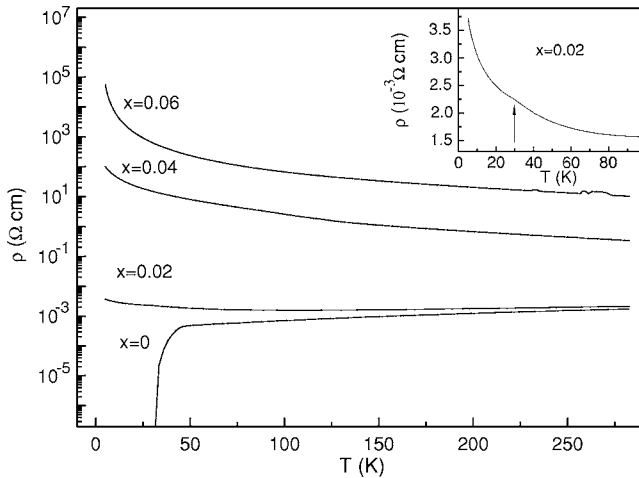


FIG. 11. The temperature dependence of the resistivity of $\text{La}_{1.85}\text{Sr}_{0.15}\text{Cu}_{1-x}\text{Ti}_x\text{O}_4$ ($0 \leq x \leq 0.06$). The inset is the enlarged view for $x=0.02$.

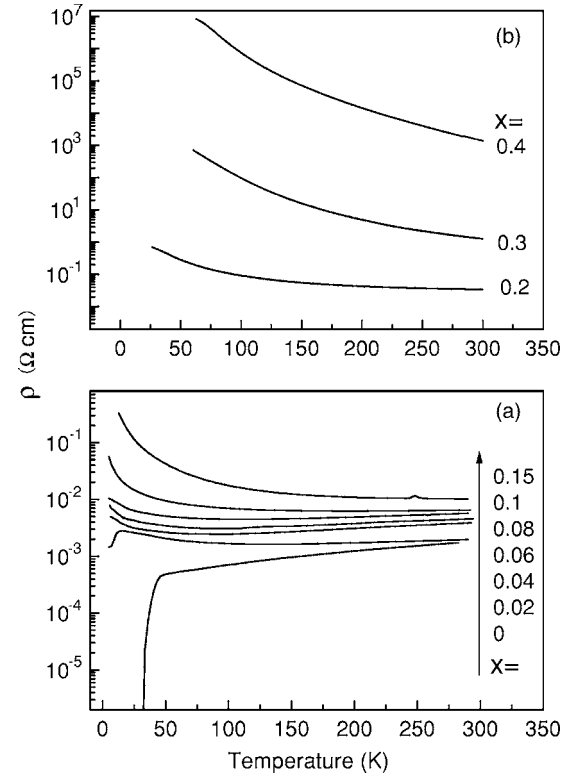


FIG. 12. The temperature dependence of the resistivity of $\text{La}_{1.85-2x}\text{Sr}_{0.15+2x}\text{Cu}_{1-x}\text{Ti}_x\text{O}_4$ ($0 \leq x \leq 0.4$).

crease of hole carrier concentration in the CuO_2 plane. In double-doped samples, the hole carrier concentrations maintain unchanged due to the compensative effect. For the two systems, it is interesting that although the magnetization exhibits diamagnetism behavior in the $\text{La}_{1.85}\text{Sr}_{0.15}\text{Cu}_{1-x}\text{Ti}_x\text{O}_4$ system at $0.02 \leq x \leq 0.04$ and in the $\text{La}_{1.85-2x}\text{Sr}_{0.15+2x}\text{Cu}_{1-x}\text{Ti}_x\text{O}_4$ system at the doping level $0.04 \leq x \leq 0.1$ (see Figs. 7 and 8), the trace of superconductivity cannot be recognized electrically here. We consider that the reason for the absence of the temperature of zero resistivity may be attributed to the decrease of the superconducting volume fraction due to the addition of dopants, which can be observed from the ZFC results in our experiments. That is when the fraction of the superconductor is reduced to a critical value the superconducting phase cannot connect to each other and form a conductive path resulting in the absence of the temperature of zero resistivity. In other words, the superconductivity is immersed by the higher resistivity. Thus, the zero resistivity behaviour is not observed.

In the curves of resistivity versus temperature, the negative $d\rho/dT$ at lower temperature was usually regarded as evidence of the localized nature of the charge carriers.²⁷ The temperature dependence of resistivity fitted by variable range hopping model²⁸ (VRH) [$\rho = \exp(T_0/T)^{1/4}$] for the samples with $0.04 \leq x \leq 0.4$ is shown in Fig. 13. The results show that ρ - T curves can be well described by the VRH model. The fitting parameter T_0 , which is a characteristic temperature related to the localization length ξ and the density of states $N(E_F)$ in the vicinity of the Fermi energy level, i.e., $\kappa_B T_0 \approx 21/[\xi^3 N(E_F)]$, is shown in Table I. From Table I, it is

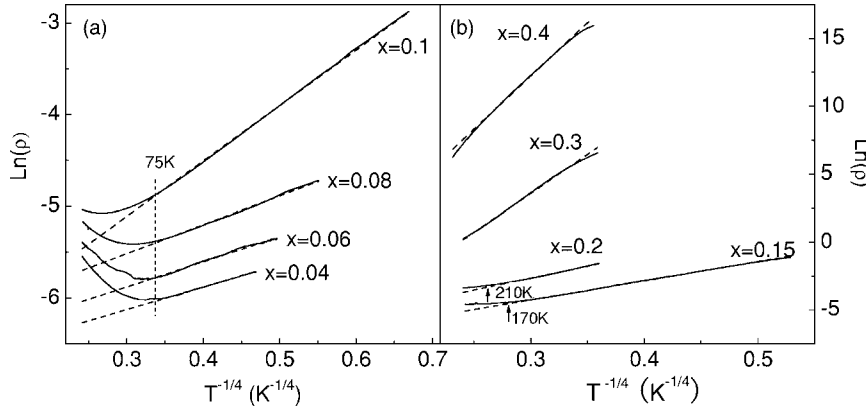


FIG. 13. The variable-range hopping fitting of resistivity curves for $\text{La}_{1.85-2x}\text{Sr}_{0.15+2x}\text{Cu}_{1-x}\text{Ti}_x\text{O}_4$ ($0.04 \leq x \leq 0.4$); the dashed lines represent the fitting data.

found that the T_0 value increases obviously with the increase of Ti content, implying the decrease of the localization length and the reduction of the carrier mobility, which is in accordance with the magnetic and electronic transport properties for the samples

E. Origin of suppressing superconductivity

From the above experimental results we notice that the doping of Ti ions suppresses the superconductivity. It is widely accepted that the Ti element is generally a stable tetravalent in transition-metal oxides. Moreover Ti^{4+} is a nonmagnetic cation because the electron configuration of the Ti^{4+} ion is $3p^63d^0$. In the Ti-doped samples, there is no exchange interaction between $2p$ orbit of O^{2-} and $3d$ orbit of Ti^{4+} . The Ti ions are distributed in the parent CuO_2 plane individually and randomly and act as nonmagnetic impurities. Xiao *et al.*⁷ and Tarascon *et al.*⁸ have argued that nonmagnetic dopants such as Zn^{2+} , Ga^{3+} , Al^{3+} have an inert full-shell structure ($3d^0$ and $3p^6$) and their main role is to locally remove the spin of Cu^{2+} ($3d^9$) ($s=1/2$), consequently, breaking the compensation and creating a net spin of $S=1/2$. They consider that it is the staggered magnetic moments that cause the magnetic pair breaking and depress the superconductivity. As a result, a similar moment can also be induced by doped Ti^{4+} at the Cu^{2+} site.

According to the conventional Abrikosov and Gork'ov theory²⁹ this magnetic pair-breaking effect can be expressed in the AG equation given as

$$\ln \frac{T_c}{T_{c0}} = \psi\left(\frac{1}{2}\right) - \psi\left(\frac{1}{2} + \frac{2J^2S(S+1)N(E_F)x}{2\kappa_B T_c}\right), \quad (3)$$

where T_{c0} is the value of T_c at $x=0$. J is the constant for the exchange interaction between the hole spin and the spin of the $3d$ metal ions. S is the spin quantum number of the $3d$ element after substitution. The quantity $N(E_F)$ is the density of states at the Fermi level, and ψ is the differential of the Γ function. When x is small, Eq. (3) can be interpreted as

$$T_{c0} - T_c = \frac{\pi^2 J^2 S(S+1)N(E_F)x}{2\kappa_B}. \quad (4)$$

If $N(E_F)$ remains constant with increasing doping content, formula (4) can be described as

$$T_{c0} - T_c = Ax. \quad (5)$$

Figure 14 shows the Ti content x dependence of T_c^{onset} for our results as compared to the prediction of the magnetic pair-breaking mechanism which is denoted by the dashed line. It is obvious that the depression of T_c does not obey formula (5) for samples with $x \leq 0.04$. However, according to formula (5), the T_c^{onset} value would drop to zero at the doping content $x=0.122$, while the experimental results indicate that the superconducting transitions disappear for the sample with $x=0.06$. These results indicate that the suppression of superconductivity does not result from the magnetic pair-breaking effects for the single-doped samples. Additionally, if the magnetic pair-breaking theory is correct in describing the high temperature superconductivity, the dopant concentration x_c of losing superconductivity in both the single-doped and double-doped LSCO should be the same. Unfortunately, this is not the case, as we describe above; there is a noticeable difference of dopant concentration x_c between the single-doped samples and the double-doped samples. These results indicate that the suppression of superconductivity cannot be attributed to the magnetic pair-breaking effect in the two series of samples. It is generally accepted that the free holes, which are active charge carriers responsible for superconductivity, exist in the CuO_2 plane. We consider that the doping of high-valence Ti^{4+} not only blocks the Cu-O-Cu long-range hybridization, but also influences the carrier in the nearby Cu-O-Cu path. When the high-valence Ti^{4+} impurity elements are introduced into the CuO_2 plane, the local number of the electrons around the impurity atoms is enhanced. The interaction between the electrons of the impurity atoms

TABLE I. The fitting parameter of $\text{La}_{1.85-2x}\text{Sr}_{0.15+2x}\text{Cu}_{1-x}\text{Ti}_x\text{O}_4$ ($0.04 \leq x \leq 0.4$) samples.

Parameter	$x=0.04$	$x=0.06$	$x=0.08$	$x=0.1$	$x=0.15$	$x=0.2$	$x=0.3$	$x=0.4$
T_0 (K)	3.63×10	5.62×10	9.74×10	1.34×10^3	3.99×10^4	1.05×10^5	1.08×10^7	3.82×10^7

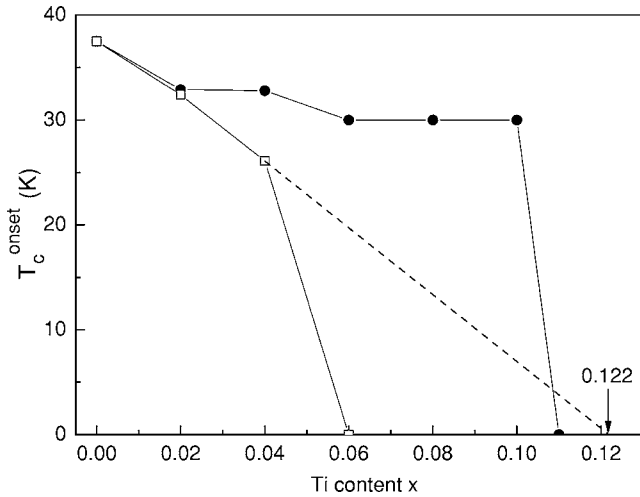


FIG. 14. Variation of T_c^{onset} with the Ti doping content x (hollow squares: $\text{La}_{1.85}\text{Sr}_{0.15}\text{Cu}_{1-x}\text{Ti}_x\text{O}_4$ samples; solid circles: $\text{La}_{1.85-2x}\text{Sr}_{0.15+2x}\text{Cu}_{1-x}\text{Ti}_x\text{O}_4$ samples).

and the holes of the neighboring oxygen atoms will cause the holes to localize and lose their itinerancy and prevents them from condensing into pairs; then the superconductivity is suppressed. For singly doped $\text{La}_{1.85}\text{Sr}_{0.15}\text{Cu}_{1-x}\text{Ti}_x\text{O}_4$ samples, the doping of high-valence Ti ions into Cu sites leads to a reduction in carrier concentration, while for doubly doped $\text{La}_{1.85-2x}\text{Sr}_{0.15+2x}\text{Cu}_{1-x}\text{Ti}_x\text{O}_4$ samples, due to the charge carrier compensation effect, this effect is weakened. Thus the suppression of superconductivity is less severe in double-doped samples than in single-doped samples.

It is well known that the undoped compound La_2CuO_4 is an insulating antiferromagnet where the spin moments on adjacent Cu^{2+} ions are antiparallel.³⁰ The itinerant holes introduced by doping of Sr^{2+} depresses the superexchange interaction of $\text{Cu}^{2+}\text{-O-Cu}^{2+}$ and consequently destroys the long-range AFM correlation. As a result, the relationship between the antiferromagnetism and the superconductivity in the CuO_2 has been the focus of the cuprate superconductivity research. Previously we have investigated the high-valence Mn doped $\text{La}_{1.85}\text{Sr}_{0.15}\text{CuO}_4$ (LSCO),⁴ where the double-doped $\text{La}_{1.85-2x}\text{Sr}_{0.15+2x}\text{Cu}_{1-x}\text{Mn}_x\text{O}_4$ was used and we observed the superconductivity in competition with antiferromagnetic correlation between Mn ions which are confirmed to be tetravalent. However, this competition has not been observed in the high-valence Ti doped $\text{La}_{1.85-2x}\text{Sr}_{0.15+2x}\text{Cu}_{1-x}\text{Ti}_x\text{O}_4$ system. As we know, both the $(\text{La}/\text{Sr})_2\text{CuO}_4$ and the $(\text{La}/\text{Sr})_2\text{MnO}_4$ have the same K_2NiF_4 structure and can exist independently. When prepared by the conventional solid-state reaction method, it is much possible for the $(\text{La}/\text{Sr})_2\text{MnO}_4$ to exist independently in the $(\text{La}/\text{Sr})_2\text{CuO}_4$, so the Mn-O-Mn and Cu-O-Cu can exist in

the same planes. Naturally, Mn ions easily close to each other and form antiferromagnetic correlation in the double-doped $\text{La}_{1.85-2x}\text{Sr}_{0.15+2x}\text{Cu}_{1-x}\text{Mn}_x\text{O}_4$ system. However, it is different in the high-valence Ti doped $\text{La}_{1.85-2x}\text{Sr}_{0.15+2x}\text{Cu}_{1-x}\text{Ti}_x\text{O}_4$ system. Moreover Ti^{4+} is a non-magnetic cation because the electron configuration of the Ti^{4+} ion is $3p^63d^0$. In the Ti-doped samples, there is no exchange interaction of p holes with the $3d$ electrons in the $\text{O}^{2-}\text{-L-Ti}^{4+}$ (L is a $2p$ hole in oxygen) groups. When Ti^{4+} ions become adjacent with other Ti^{4+} ions, a strong localized stress come into being, this induces a larger aberrance. Therefore, the Ti ions would be distributed in the parent CuO_2 plane individually and randomly.

IV. CONCLUSIONS

In summary, the effects of Ti doping of $\text{La}_{1.85}\text{Sr}_{0.15}\text{CuO}_4$ have been studied by means of measurements of the magnetic susceptibility and electrical transport. We obtain pure phase samples of $\text{La}_{1.85}\text{Sr}_{0.15}\text{Cu}_{1-x}\text{Ti}_x\text{O}_4$ at doping levels $x \leq 0.06$, while by virtue of the double-doping technique, we successfully synthesized pure phase samples of $\text{La}_{1.85-2x}\text{Sr}_{0.15+2x}\text{Cu}_{1-x}\text{Ti}_x\text{O}_4$ ($0 \leq x \leq 0.4$). This indicates that the double-doping process is effective in improving the doping level at the Cu site with high-valence transition elements due to the compensation of charge carriers in the CuO_2 plane. The magnetization measurements indicate that the critical Ti doping level (above which the superconductivity is suppressed) of double-doped samples are much higher than that of the single-doped samples. For the single-doped samples, the diamagnetic signal is observed at the doping levels $x \leq 0.04$, while for the double-doped samples the diamagnetism can survive upon replacing 10% of planar Cu ions with Ti ions. The resistivity measurements show that the depression of T_c is less sharp in double-doped samples than in single-doped samples. For the single-doped samples, at about 40 K which is little higher than the T_c for $x=0$, the resistivity of $x=0.06$ is about six orders of magnitude higher than that of $x=0$. While for the double-doped samples, at about 40 K, the resistivity of $x=0.06$ is only one order of magnitude higher than that of $x=0$. Those experimental results are understood in terms of the charge carrier compensation effect. Doping with Ti leads to the localization of hole carriers. The suppression of superconductivity is most likely due to the localization of hole carriers and not due to the pair-breaking effect induced by nonmagnetic disorder.

ACKNOWLEDGMENTS

This work is supported by the Natural Science Foundation of China (Grant No. 10334009), the Ministry of Science and Technology of China (Grant No. NKBRSF-G19990646), and the fundamental Bureau of Chinese Academy of Sciences.

*Electronic address: Zhangyh@ustc.edu.cn

- ¹J. G. Bednorz and K. A. Müller, Z. Phys. B: Condens. Matter **64**, 189 (1986).
- ²R. Kadono, K. Ohishi, A. Koda, R. S. Saha, W. Higemoto, M. Fujita, and K. Yamada, J. Phys. Soc. Jpn. **74**, 2806 (2005).
- ³R. Klingeler, N. Tristan, B. Buchner, M. Hucker, U. Ammerahl, and A. Revcolevschi, Phys. Rev. B **72**, 184406 (2005).
- ⁴C. Zhang and Y. Zhang, Phys. Rev. B **68**, 054512 (2003).
- ⁵C. X. Wang, Y. P. Sun, and Y. H. Zhang, Supercond. Sci. Technol. **19**, 122 (2006).
- ⁶N. Ishikawa, N. Kuroda, H. Ikeda, and Yoshizaki, Physica C **203**, 284 (1992).
- ⁷G. Xiao, M. Z. Cieplak, J. Q. Xiao, and C. L. Chien, Phys. Rev. B **42**, 8752 (1990).
- ⁸J. M. Tarascon, L. H. Greene, P. Barboux, W. R. McKinnon, G. W. Hull, T. P. Orlando, K. A. Delin, S. Foner, and E. J. McNiff, Jr., Phys. Rev. B **36**, 8393 (1987).
- ⁹N. Bulut, D. Hone, D. J. Scalapino, and E. Y. Loh, Phys. Rev. Lett. **62**, 2192 (1989).
- ¹⁰X. Gaojie, M. Zhiqiang, J. Hao, Y. Hongjie, W. Bin, L. Dengpan, and Z. Yuheng, Phys. Rev. B **59**, 12090 (1999).
- ¹¹B. I. Kochelaev, L. Kan, B. Elschner, and S. Elschner, Phys. Rev. B **49**, 13106 (1994).
- ¹²G. Xiao, A. Bakhshai, M. Z. Cieplak, Z. Tesanovic, and C. L. Chien, Phys. Rev. B **39**, 315 (1989).
- ¹³J. Takeda, T. Nishikawa, and M. Sato, Physica C **231**, 293 (1994).
- ¹⁴G. Xiao, P. Xiong, and M. Z. Cieplak, Phys. Rev. B **46**, 8687 (1992).
- ¹⁵C. J. Zhang and Y. H. Zhang, J. Phys.: Condens. Matter **14**, 9659 (2002).
- ¹⁶D. B. Wiles and R. A. Young, J. Appl. Crystallogr. **14**, 149 (1981).
- ¹⁷T. Brun, M. Grimsditch, K. E. Gray, R. Bhadra, V. Maroni, and C. K. Loong, Phys. Rev. B **35**, 8837 (1987).
- ¹⁸R. Henn, J. Kircher, and M. Cardona, Physica C **269**, 99 (1996).
- ¹⁹M. Stavola, R. J. Cava, and E. A. Rietman, Phys. Rev. Lett. **58**, 1571 (1987).
- ²⁰T. Blundell, *Magnetism in Condensed Matter* (Oxford University Press, Oxford, 2001).
- ²¹J. K. Furdyna and J. Kossut, *Diluted Magnetic Semiconductors*, Vol. 25 in Semiconductors and Semimetals (Academic, New York, 1988).
- ²²S. de Brion, F. Ciorcas, G. Chouteau, P. Lejay, P. Radaelli, and C. Chaillout, Phys. Rev. B **59**, 1304 (1999).
- ²³T. Hasegawa, K. Kishio, M. Aoki, N. Ooba, K. Kitazawa, K. Fueki, S. Uchida, and S. Tanaka, J. Appl. Phys. **26**, L337 (1987).
- ²⁴W. Kang, H. J. Schulz, D. Jérôme, S. S. P. Parkin, J. M. Bassat, and Ph. Odier, Phys. Rev. B **37**, 5132 (1988).
- ²⁵M. Z. Cieplak, G. Xiao, A. Bakhshai, and C. L. Chien, Phys. Rev. B **39**, 4222 (1989).
- ²⁶G. Xiao, J. Q. Xiao, C. L. Chien, and M. Z. Cieplak, Phys. Rev. B **43**, 1245 (1991).
- ²⁷H. Wu, L. Lin, Y. D. Sun, L. T. Ding, W. X. Wang, and Y. H. Zhang, Supercond. Sci. Technol. **18**, 277 (2005).
- ²⁸A. Sundaresan, A. Maignan, and B. Raveau, Phys. Rev. B **56**, 5092 (1997).
- ²⁹A. A. Abrikosov and L. P. Gor'kov, Sov. Phys. JETP **12**, 1243 (1961).
- ³⁰D. Vaknin, S. K. Sinha, D. E. Moncton, D. C. Johnston, J. M. Newsam, C. R. Safinya, and H. E. King, Jr., Phys. Rev. Lett. **58**, 2802 (1987).